



ELSEVIER

17 May 2001

PHYSICS LETTERS B

Physics Letters B 507 (2001) 1–6

www.elsevier.nl/locate/npe

First positron cooling of antiprotons

G. Gabrielse^a, J. Estrada^a, J.N. Tan^a, P. Yesley^a, N.S. Bowden^a, P. Oxley^a, T. Roach^{a,1},
C.H. Storry^a, M. Wessels^a, J. Tan^a, D. Grzonka^b, W. Oelert^b, G. Schepers^b,
T. Seifick^b, W.H. Breunlich^c, M. Cargnelli^c, H. Fuhrmann^c, R. King^c, R. Ursin^c,
J. Zmeskal^c, H. Kalinowsky^d, C. Wesdorp^e, J. Walz^{f,2}, K.S.E. Eikema^f, T.W. Hänsch^f

^a Department of Physics, Harvard University, Cambridge, MA 02138, USA

^b IKP, Forschungszentrum Jülich GmbH, 52425 Jülich, Germany

^c Institute for Medium Energy Physics, Boltzmannngasse 3, 1090 Vienna, Austria

^d Institut für Strahlen-und Kernphysik, University of Bonn, 53115 Bonn, Germany

^e FOM Institute for Atomic and Molecular Physics, Kruislaan 407, 1098 SJ, 1098 SJ, Amsterdam, Netherlands

^f Max-Planck-Institut für Quantenoptik, Hans-Kopfermann-Strasse 1, 85748 Garching, Germany

Received 28 March 2001; accepted 3 April 2001

Editor: L. Montanet

Abstract

Positrons are used to cool antiprotons for the first time. The oppositely charged positrons and antiprotons are first simultaneously accumulated in separate Penning trap volumes, and then are spatially merged in a nested Penning trap. The antiprotons cool until they reach a low relative velocity with respect to the cold positrons, the situation expected to be optimal for the production of cold antihydrogen. © 2001 Published by Elsevier Science B.V.

Simultaneous electrical signals from separated positrons and antiprotons, first at CERN [1] then at Fermilab [2], confirmed the fleeting existence of several antihydrogen atoms, the first observed atoms made entirely of antimatter. The small number and brief existence of these bound states of positrons and antiprotons, traveling at nearly the speed of light, make any comparison of the properties of antihydrogen and hydrogen at an interesting level of accuracy to be extremely unlikely.

Cold antihydrogen atoms (at temperatures not far from absolute zero) have not yet been observed, but offer the exciting prospect of antihydrogen captured in a magnetic trap [3] long enough to use lasers to probe for any difference between antihydrogen and hydrogen. The ingredients of cold antihydrogen have been previously confined in the same trap structure [4]. This letter from the ATRAP Collaboration [5] reports the first observation of positron cooling of antiprotons, the closest approach yet to the production of cold antihydrogen. The antiprotons cool to a low relative velocity with respect to the positrons, a condition expected to facilitate the production of cold antihydrogen.

The antiprotons come from CERN's new Antiproton Decelerator (AD) [6]. Late in 2000 the AD started delivering 330 ns pulses of 5 MeV antiprotons, with

E-mail address: gabrielse@physics.harvard.edu (G. Gabrielse).

¹ New address: College of the Holy Cross, Worcester, MA 01610, USA.

² New address: CERN, 1211 Geneva 23, Switzerland.

3×10^7 antiprotons per pulse in the best case. This is a hundred times fewer antiprotons per pulse than was available from the three-storage-ring complex (ACOL, AA and LEAR) that the AD replaced. However, pulses are sent much more often — every 110 seconds — and can be accumulated more inexpensively in a trap [7] than in a complex involving several storage rings.

The 5 MeV antiprotons from the AD are accumulated at 4.2 K, an energy reduction greater than 10^{10} . The required techniques to slow, trap, cool, and accumulate these antiprotons [7–10] were recently reviewed [11]. They were developed by the TRAP Collaboration, the predecessor of ATRAP. Positrons from a 110 mCi ^{22}Na source are also slowed, trapped, cooled and accumulated at 4.2 K. High Rydberg positronium is formed, and then ionized and captured at a rate that exceeds the recent first demonstration of this technique [12] by a factor of 27.

The intricate trap apparatus (Fig. 1) within which the antiprotons and positrons are captured, cooled and accumulated includes 32 ring electrodes stacked vertically. A 6 Tesla magnetic field (from a superconducting solenoid) is parallel to the central symmetry axis of the trap electrodes. Each of these electrodes is made of gold-plated OFE copper with a 1.2 cm inner diameter. Appropriate potentials on any three (or five) adjacent electrodes form a Penning trap for charged particles [13]. The electrodes are within a copper vacuum enclosure sealed with indium and cooled to 4.2 K via a thermal contact to liquid helium. The long (> 3.2 months) lifetime of trapped antiprotons within a simi-

lar container established a pressure less than 5×10^{-17} Torr [10]. (No magnetic trap for antihydrogen was used in this first demonstration.)

A rotatable electrode separates an upper region (where positrons are trapped and accumulated) from a lower region (where antiprotons are trapped and accumulated at the same time). This unusual electrode can be rotated while at low temperature, while within the extremely high vacuum, and in the presence of a high field. The 6 Tesla field, and a current sent through coils attached to the electrode, generate the required torque. In its closed position this electrode prevents antiprotons from disrupting the positron loading, as observed earlier [4,12]. After the accumulations, the electrode is rotated to its open position to allow trapped positrons to join the antiprotons.

The trap is surrounded by layers of detectors (Fig. 1) that are just outside a thin copper vacuum enclosure (not shown in the figure). The BGO crystals, operated at 77 K, will be used later to detect photons from positron annihilation. Three layers of scintillating fibers, also near 77 K, detect charged pions from antiproton annihilation. The two inner layers are 1.5 mm diameter fibers in about 38.5 degree helices, offset to close the gaps between fibers. The 1.9 mm diameter fibers in the outer layer are vertical, and parallel to the axis of the trap. The superconducting solenoid that produces the vertical magnetic field, and its dewars, surround the scintillating fibers. A double layer of segmented plastic scintillators, surrounding the dewar, also detects pions from antiproton annihilation.

A coincidence of two of the three scintillating fiber layers detects an antiproton annihilation within the trap region with essentially 100% efficiency, but with a background counting rate of 55/s. A coincidence of the two outer scintillators detects an antiproton annihilation within the trap region with an efficiency of 50% but with a background counting rate of 75/s. A coincidence of both signals reduces the background counting rate to 3/s.

The pulsed antiproton beam from the AD is directed upward into our apparatus, where the antiprotons are centered within approximately a 4 mm diameter using a parallel plate avalanche detector operated in ionization mode. The energy of these antiprotons is varied slightly by changing the amount of SF_6 mixed with He in a 1.5 cm long gas cell, to maximize the

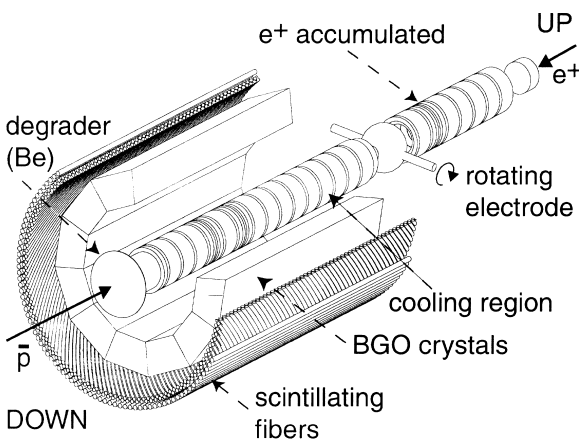


Fig. 1. Overview of the trap and detectors.

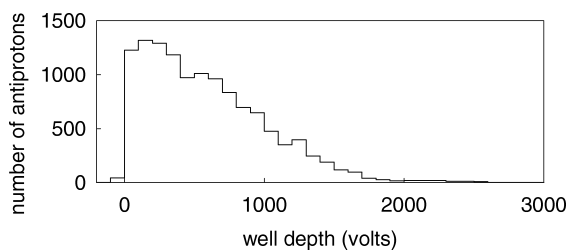


Fig. 2. Energy spectra for 12000 of the first antiprotons trapped from a single pulse of antiprotons from the AD.

number slowed below 4 keV in the 125 μm thick beryllium degrader that follows the cell [9]. These slowed antiprotons are reflected by a -4 kV potential applied to an electrode just before the rotatable one. Before they can return to the degrader, its potential is pulsed to -4 kV to capture the antiprotons [8].

Up to 12000 antiprotons are captured in this 4 kV trap from a single pulse of antiprotons from the AD, an efficiency of about 5×10^{-4} , consistent with earlier measurements in a similar trap [11]. The energy of the trapped antiprotons is analyzed by slowly reducing the depth of the potential well that confines them (Fig. 2), and counting the annihilations of antiprotons that leave the trap. Because the energy spread of antiprotons emerging from the degrader is very wide compared to the energies we can capture, the number of trapped particles increases approximately linearly with the depth of the trapping well. A linear extrapolation suggests that in a larger trap with 20 kV potentials we could capture up to 40000 antiprotons per pulse.

We precool the antiprotons (before they interact with the separately accumulated positrons) by colliding them with 4.2 K electrons [7], the only stable matter species that can collide with antiprotons without annihilating them. The electrons are preloaded into several small wells within the trap before the antiprotons arrive. The electrons themselves cool rapidly via the spontaneous emission of synchrotron radiation until they reach equilibrium with the surrounding electrodes at 4.2 K. The captured antiprotons cool in tens of seconds as they travel back and forth through the electrons, transferring their energy to the cold electrons with which they collide. Up to 100% of the trapped antiprotons cool into the wells occupied by the cold electrons.

Once the antiprotons reside in the small wells with the cooling electrons we can inject and cool

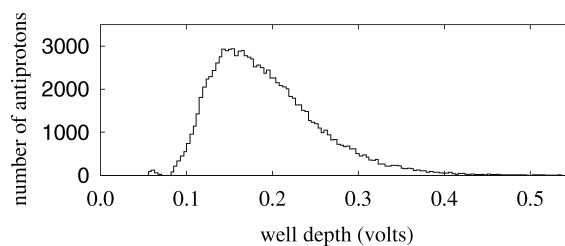


Fig. 3. Energy spectrum for 106000 of the first antiprotons electron-cooled and stacked at the AD.

more pulses of antiprotons, using the same cooling electrons. Our automated apparatus routinely stacks more than 10^5 antiprotons (Fig. 3) while unattended. We have yet to investigate the accumulation of more antiprotons, but it should be possible since we are far from the space charge and Brillouin limits.

When we have stacked the desired number of antiprotons we slowly change the potentials on the trap electrodes to transfer all the antiprotons and electrons into one potential well within one electrode. Switching this potential well off for 300 ns then ejects the electrons, while the more massive antiprotons do not accelerate sufficiently to leave the trap.

Positrons accumulate in the upper trap region at the same time that antiprotons accumulate below. The new and efficient method for accumulating large numbers of 4.2 K positrons [12] is the only one yet demonstrated. Since these positrons accumulate directly in the highest field region, at 6 Tesla, we avoid the magnetic bounce that would reduce the number of positrons able to move from a weak to a strong magnetic field.

The positrons come from a 110 mCi ^{22}Na source that is 3 mm in diameter. This source is precooled to near 77 K and is lowered 2 m from its lead shielding enclosure, down through the helium dewar needed to keep the trap cold, until it settles against the 4.2 K trap enclosure. Positrons, whose energy distribution has a 0.5 MeV endpoint, follow magnetic field lines and enter the trap vacuum through a 10 μm thick Ti window. Some of them slow as they enter the trapping region through a 2 μm thick single crystal of tungsten. Others slow while turning around within a thick tungsten crystal that is rotated to the trap axis when the rotatable electrode is in its closed position. Neither crystal can be struck by antiprotons when the rotatable electrode is in its closed position. This leaves

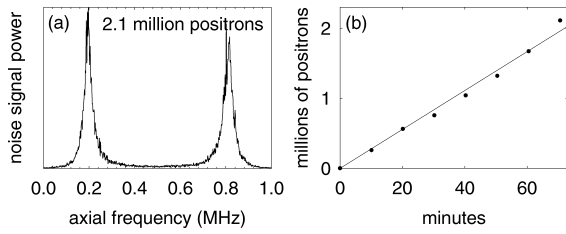


Fig. 4. (a) Electrical signal from 2.1 million trapped positrons. (b) Positrons accumulate at a rate 27 times higher than reported in a recent introduction to the technique.

undisturbed the essential layer of absorbed gas on the thin crystal of tungsten, without which positron loading ceases [4,12].

Slow positrons that pick up electrons while leaving the thin crystal form Rydberg positronium atoms. These atoms travel parallel to the axis of the trap until they are ionized by the electric field of the trap well, and captured. The frequency spacing of the two peaks in the electrical signal induced across an RLC circuit attached to the trap reveals the number of accumulated positrons. Fig. 4(b) shows approximately 2 million positrons accumulating in an hour, a 27-fold increased rate compared to our recent report [12] announcing the method. Normalized to the source strength, the maximum rate we observe is $1.4 \times 10^4 e^+ h^{-1} mCi^{-1}$. This is a bit smaller than our previous rate, presumably because the larger source diameter compromises the positron accumulation. Switching the rotatable electrode to its open position allows positrons to be moved into the lower section of the trap with the antiprotons, with a transfer efficiency of 80% or higher.

Four radiofrequency detectors nondestructively detect the number of positrons (Fig. 4(a)) and other trapped particles, and damp oscillations of these particles. The particle motions induce detectable currents in resonant RLC circuits attached to trap electrodes, and the energy dissipated in these circuits is removed from the particle motions. Positron and electron motion along the magnetic field direction are so damped, as is similar antiproton (or proton) motion (Fig. 5), and antiproton (or proton) cyclotron motion. Positron and electron cyclotron motion damps via the spontaneous emission of synchrotron radiation, while magnetron drift motion of all particles can be reduced by sideband cooling [13].

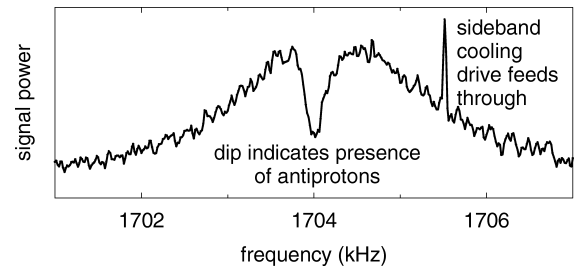


Fig. 5. Nondestructive electrical signal from trapped antiprotons which are cooled by the detector.

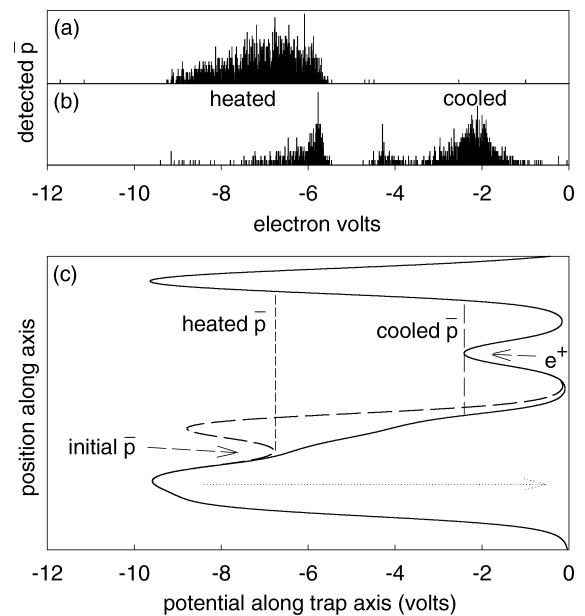


Fig. 6. (a) Uncooled antiproton spectrum. (b) Cooled antiproton spectrum shows some antiprotons are not cooled. (c) Potential wells for the positrons and antiprotons.

Positron cooling of antiprotons is similar in principle to electron cooling of antiprotons. The motional energy of the trapped antiprotons is transferred to lighter trapped particles by Coulomb collisions, and the lighter particles cool rapidly via synchrotron radiation. There are two important differences in practice. First, since the positrons and antiprotons have an opposite sign of charge, they cannot be confined in the same Penning trap well. Our solution is the nested Penning trap [14] (Fig. 6(c)). The device and technique were investigated earlier with electrons and protons [15] though with far fewer electrons than the

number of positrons used here. The second difference is the obvious technical challenge of producing and manipulating two antimatter species, rather than two matter species.

A potential well containing cold antiprotons and electrons is adiabatically elevated as shown in Fig. 6(c). The antiprotons are launched into the nested trap, and given kinetic energy by pulsing the dashed potential curve to the solid curve. Simultaneously, the potential barrier at the opposite end of the nested well is pulsed near zero volts to encourage any electrons confined with the antiprotons to leave the well. Both barriers are restored to full height after 1.5 μs , before the slower antiprotons can make it from the launching point to the turning point. The antiprotons are now in a nearly symmetrical nested well structure.

Two minutes after the antiprotons are injected into the nested well, the energy distribution of the trapped antiprotons is analyzed by slowly lowering the potential barrier nearest the launch point (dotted arrow in Fig. 6(c)). When no positrons are present in the nested trap, Fig. 6(a) shows the number of annihilations of antiprotons released from the trap as a function of the remaining barrier height. In this example about 4000 antiprotons had kinetic energies distributed around 7 eV relative to the bottom of the potential well.

To demonstrate positron cooling we repeat this process but with approximately 250000 positrons preloaded into the inverted central well that is nested within the longer outer well. These positrons cool via synchrotron radiation to thermal equilibrium with their 4.2 K environment in only 0.1 seconds. They are collected into a volume that is a couple of millimeters in radius and length, with a density of $7 \times 10^6 \text{ cm}^{-3}$. Antiprotons are launched into the nested trap exactly as before. The antiprotons that pass through the positron cloud are cooled by collisional transfer of energy to the positrons.

When we analyze the antiproton energy as before we see in Fig. 6(b) that most of the antiprotons have cooled to approximately the same level in the well that is occupied by the positrons. They do not cool below this energy because the cooling stops when the antiprotons have insufficient energy to reenter the positron cloud. There are also some antiprotons that are not cooled, presumably because they are located away from the center axis of the trap where there are

no cold positrons. The number of uncooled antiprotons could likely be reduced by sideband cooling of the antiprotons before their launch. We do not yet understand the small intermediate energy peak of partially cooled antiprotons.

The cooled antiprotons have a low relative velocity with respect to the cold positrons that cooled them. A low relative velocity is one condition under which antihydrogen formation processes (e.g., radiative recombination and three body recombination) are expected to have their highest rates. These rates are nonetheless very small so that observing these processes will take much time and care. In addition, the electric fields of the trap will ionize any high Rydberg state produced by the latter process.

Much remains to be done before cold antihydrogen is observed and precise laser spectroscopy is performed. However, this first positron cooling of antiprotons demonstrates that it is possible to make the ingredients of cold antihydrogen interact at very low energies, and is the closest approach yet to cold antihydrogen.

Acknowledgements

We are grateful to CERN for constructing the new AD so that studies of cold antihydrogen could be carried out, to Japan, Germany, the United States, and Italy for the needed external support, and to the CERN PS Division and the AD team for making the AD deliver cooled antiprotons starting in July 2000. Since this is the first publication of the ATRAP Collaboration, we are especially grateful to our home institutions for the technical support and effort devoted to the construction of the ATRAP apparatus. This work was supported by the NSF, AFOSR, the ONR of the US, the German BMBF, the Austrian Academy of Sciences, and the FOM/NWO of The Netherlands.

References

- [1] G. Baur et al., *Phys. Lett. B* 368 (1996) 251.
- [2] G. Blanford et al., *Phys. Rev. Lett.* 80 (1998) 3037.
- [3] G. Gabrielse, in: P. Bloch, P. Paulopoulos, R. Klapisch (Eds.), *Fundamental Symmetries*, Plenum, New York, 1987, p. 59.

- [4] G. Gabrielse, D. Hall, T. Roach, P. Yesley, A. Khabbaz, J. Estrada, C. Heimann, H. Kalinowsky, *Phys. Lett. B* 455 (1999) 311.
- [5] <http://hussle.harvard.edu/~atrap>.
- [6] S. Maury, *Hyperfine Int.* 109 (1997) 43.
- [7] G. Gabrielse, X. Fei, L. Orozco, R. Tjoelker, J. Haas, H. Kalinowsky, T. Trainor, W. Kells, *Phys. Rev. Lett.* 63 (1989) 1360.
- [8] G. Gabrielse, X. Fei, K. Helmerson, S. Rolston, R. Tjoelker, T. Trainor, H. Kalinowsky, J. Haas, W. Kells, *Phys. Rev. Lett.* 57 (1986) 2504.
- [9] G. Gabrielse, X. Fei, L. Orozco, S. Rolston, R. Tjoelker, T. Trainor, J. Haas, H. Kalinowsky, W. Kells, *Phys. Rev. A* 40 (1989) 481.
- [10] G. Gabrielse, X. Fei, L. Orozco, R. Tjoelker, J. Haas, H. Kalinowsky, T. Trainor, W. Kells, *Phys. Rev. Lett.* 65 (1990) 1317.
- [11] G. Gabrielse, *Adv. At. Mol. Opt. Phys.* 45 (2000) 1.
- [12] J. Estrada, T. Roach, J. Tan, P. Yesley, D. Hall, G. Gabrielse, *Phys. Rev. Lett.* 84 (2000) 859.
- [13] L.S. Brown, G. Gabrielse, *Rev. Mod. Phys.* 58 (1986) 233.
- [14] G. Gabrielse, S. Rolston, L. Haarsma, W. Kells, *Phys. Lett. A* 129 (1988) 38.
- [15] D. Hall, G. Gabrielse, *Phys. Rev. Lett.* 77 (1996) 1962.